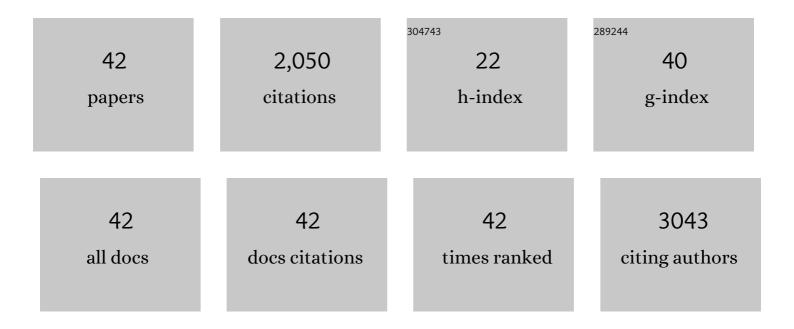
## Guodong Wei

List of Publications by Year in descending order

Source: https://exaly.com/author-pdf/6217733/publications.pdf Version: 2024-02-01



#	Article	IF	CITATIONS
1	Bioinspired surface-enhanced Raman scattering substrate with intrinsic Raman signal for the interactive SERS detection of pesticides residues. Spectrochimica Acta - Part A: Molecular and Biomolecular Spectroscopy, 2022, 270, 120800.	3.9	6
2	Simulation and design of dual-band quantum dot infrared photodetector based on metal grating structure. AIP Advances, 2022, 12, 035110.	1.3	3
3	Reusable dual-functional SERS sensor based on gold nanoflowers-modified red phosphorus nanoplates for ultrasensitive immunoassay and degradation of CA19-9. Biosensors and Bioelectronics, 2022, 207, 114148.	10.1	11
4	Robust and Low-Power-Consumption Black Phosphorus–Graphene Artificial Synaptic Devices. ACS Applied Materials & Interfaces, 2022, 14, 21242-21252.	8.0	11
5	Quantitative and recyclable SERS detection induced by tunable Raman internal standard from embedded silicon nanoparticles. Sensors and Actuators B: Chemical, 2022, 366, 131989.	7.8	13
6	Multifunctional SERS chip mediated by black phosphorus@gold-silver nanocomposites inserted in bilayer membrane for in-situ detection and degradation of hazardous materials. Journal of Colloid and Interface Science, 2022, 626, 787-802.	9.4	12
7	Development of RGO@MoS2@Ag ternary nanocomposites with tunable geometry structure for recyclable SERS detection. Sensors and Actuators B: Chemical, 2021, 339, 129856.	7.8	44
8	Flexible GO/Nb <sub>2</sub> CT <sub>x</sub> hybrid films for high-performance piezoresistive sensors. Journal Physics D: Applied Physics, 2021, 54, 424007.	2.8	4
9	Construction of Reusable PMMA–Ag/g-C <sub>3</sub> N <sub>4</sub> /Ag Hybrid Substrates with Plasmonic-Enhanced Intrinsic Raman Signals for Quantitative SERS Detection and Green Degradation. ACS Sustainable Chemistry and Engineering, 2021, 9, 12885-12898.	6.7	28
10	Nonmetallic SERS-based immunosensor byintegrating MoS2 nanoflower and nanosheet towards the direct serum detection of carbohydrate antigen 19-9. Biosensors and Bioelectronics, 2021, 193, 113481.	10.1	31
11	Surface-enhanced Raman scattering-based lateral flow immunoassay mediated by hydrophilic-hydrophobic Ag-modified PMMA substrate. Spectrochimica Acta - Part A: Molecular and Biomolecular Spectroscopy, 2021, 262, 120092.	3.9	28
12	Intrinsic Raman signal of polymer matrix induced quantitative multiphase SERS analysis based on stretched PDMS film with anchored Ag nanoparticles/Au nanowires. Chemical Engineering Journal, 2020, 381, 122710.	12.7	160
13	Quantitative SERS-Based Detection and Elimination of Mixed Hazardous Additives in Food Mediated by the Intrinsic Raman Signal of TiO <sub>2</sub> and Magnetic Enrichment. ACS Sustainable Chemistry and Engineering, 2020, 8, 16990-16999.	6.7	35
14	Enhanced Absorptivity of Quantum Dot Infrared Photodetector by Introducing of Metal Nanostructure Layer. Plasmonics, 2020, 15, 1421-1427.	3.4	1
15	Improved lateral flow strip based on hydrophilicâ^'hydrophobic SERS substrate for ultraâ^'sensitive and quantitative immunoassay. Applied Surface Science, 2020, 529, 147121.	6.1	28
16	Hierarchical NiO–CeO nanosheets self-assembly flower-like architecture: heterojunction engineering assisting for high-performance humidity sensor. Journal of Materials Science: Materials in Electronics, 2020, 31, 13229-13239.	2.2	3
17	Quantitative and Recyclable Surface-Enhanced Raman Spectroscopy Immunoassay Based on Fe <sub>3</sub> O <sub>4</sub> @TiO <sub>2</sub> @Ag Core–Shell Nanoparticles and Au Nanowire/Polydimethylsiloxane Substrates. ACS Applied Nano Materials, 2020, 3, 4610-4622.	5.0	30
18	A robust SiC nanoarray blue-light photodetector. Journal of Materials Chemistry C, 2020, 8, 6072-6078.	5.5	16

GUODONG WEI

#	Article	IF	CITATIONS
19	High Photon Absorptivity of Quantum Dot Infrared Photodetectors Achieved by the Surface Plasmon Effect of Metal Nanohole Array. Nanoscale Research Letters, 2020, 15, 98.	5.7	10
20	Polyimide/Graphene Nanocomposite Foamâ€Based Windâ€Driven Triboelectric Nanogenerator for Selfâ€Powered Pressure Sensor. Advanced Materials Technologies, 2019, 4, 1800723.	5.8	86
21	Screen-printable microscale hybrid device based on MXene and layered double hydroxide electrodes for powering force sensors. Nano Energy, 2018, 50, 479-488.	16.0	176
22	Single-crystalline integrated 4H-SiC nanochannel array electrode: toward high-performance capacitive energy storage for robust wide-temperature operation. Materials Horizons, 2018, 5, 883-889.	12.2	43
23	Binder-free Ti 3 C 2 T x MXene electrode film for supercapacitor produced by electrophoretic deposition method. Chemical Engineering Journal, 2017, 317, 1026-1036.	12.7	202
24	Facile synthesis of MnO2-Ni(OH)2 3D Ridge-like Porous Electrode Materials by Seed-induce Method for High-performance Asymmetric Supercapacitor. Electrochimica Acta, 2017, 233, 26-35.	5.2	56
25	Interface engineering of 3D BiVO <sub>4</sub> /Fe-based layered double hydroxide core/shell nanostructures for boosting photoelectrochemical water oxidation. Journal of Materials Chemistry A, 2017, 5, 9952-9959.	10.3	134
26	Cu and Ni Nanoparticles Deposited on ITO Electrode for Nonenzymatic Electrochemical Carbohydrates Sensor Applications. Electroanalysis, 2017, 29, 965-974.	2.9	5
27	Hierarchical NiCoP nanocone arrays supported on Ni foam as an efficient and stable bifunctional electrocatalyst for overall water splitting. Journal of Materials Chemistry A, 2017, 5, 14828-14837.	10.3	255
28	Flexible Supercapacitors Based on Polyaniline Arrays Coated Graphene Aerogel Electrodes. Nanoscale Research Letters, 2017, 12, 394.	5.7	67
29	Experimental and theoretical studies of nonlinear dependence of the internal resistance and electrode thickness for high performance supercapacitor. Scientific Reports, 2017, 7, 45934.	3.3	11
30	Flexible MXene–graphene electrodes with high volumetric capacitance for integrated co-cathode energy conversion/storage devices. Journal of Materials Chemistry A, 2017, 5, 17442-17451.	10.3	211
31	Magnetite hollow microspheres with a broad absorption bandwidth of 11.9 GHz: toward promising lightweight electromagnetic microwave absorption. Physical Chemistry Chemical Physics, 2017, 19, 19975-19983.	2.8	41
32	The radar absorption properties of the hollow Fe <inf>3</inf> O <inf>4</inf> microspheres synthesized by the plasma dynamic method. , 2017, , .		0
33	SERS-based immunoassay using a core–shell SiO <sub>2</sub> @Ag immune probe and Ag-decorated NiCo <sub>2</sub> O <sub>4</sub> nanorods immune substrate. RSC Advances, 2016, 6, 708-715.	3.6	19
34	Highly flexible and robust N-doped SiC nanoneedle field emitters. NPG Asia Materials, 2015, 7, e157-e157.	7.9	66
35	Fe3O4@titanate nanocomposites: novel reclaimable adsorbents for removing radioactive ions from wastewater. Journal of Materials Science: Materials in Electronics, 2015, 26, 2742-2747.	2.2	7
36	High-performance solar-blind ultraviolet photodetector based on electrospun TiO2-ZnTiO3 heterojunction nanowires. Nano Research, 2015, 8, 2822-2832.	10.4	53

GUODONG WEI

#	Article	IF	CITATIONS
37	Novel fungus–titanate bio-nanocomposites as high performance adsorbents for the efficient removal of radioactive ions from wastewater. Nanoscale, 2014, 6, 722-725.	5.6	26
38	Titanate Nanotubes as a Promising Absorbent for High Effective Radioactive Uranium Ions Uptake. Journal of Nanoscience and Nanotechnology, 2012, 12, 6374-6379.	0.9	22
39	Large-Scale Synthesis and Photoluminescence Properties of Aligned Multicore SiC–SiO <sub>2</sub> Nanocables. Journal of Nanoscience and Nanotechnology, 2010, 10, 1964-1968.	0.9	3
40	Synthesis of ZnO Nanosheets by Microwave Thermal Vapor Method. Journal of Nanoscience and Nanotechnology, 2010, 10, 2065-2069.	0.9	8
41	Large-scale synthesis and photoluminescence properties ofÂSiC networks. Applied Physics A: Materials Science and Processing, 2009, 96, 521-527.	2.3	12
42	Enhanced Photoluminescence of Water Soluble YVO <sub>4</sub> :Ln <sup>3+</sup> (Ln = Eu, Dy, Sm,) Tj ETQq	0 0 0 rgBT 3.1	/Overlock 10 73

17042-17045.